Crystal and Molecular Structure of a Potential DNA Groove-Spanning Chelate: $[MV][Pt_2(hdta)Cl_2]\cdot 4H_2O$ (MV^{2+} = 1,1′-Dimethyl-4,4′-bipyridinium, $hdta^{4-}$ = 1,6-Hexanediamine-*N*,*N*,*N*′,*N*′-tetraacetate)

Richard A. Kortes, Steven J. Geib, Fu-Tyan Lin, and Rex E. Shepherd*

Department of Chemistry, University of Pittsburgh, Pittsburgh, Pennsylvania 15260

Received January 28, 1999

Light yellow crystals of $[MV][Pt_2(hdta)Cl_2]\cdot 4H_2O$ (**1**) (MV^{2+} = 1,1′-dimethyl-4,4′-bipyridinium, $hdta^{4-}$ = 1,6-hexanediamine-*N*,*N*,*N*′,*N*′-tetraacetate) were examined by X-ray diffraction. A 0.08 × 0.24 × 0.24 nm crystal was shown to have space group *C*2/*c*, having unit cell dimensions of $a = 22.757(5)$ Å, $b = 13.566(3)$ Å, and $c = 12.120(2)$ Å and unit cell angles of $\alpha = \gamma = 90°$ and $\beta = 109.07(3)°$ with $Z = 4$. A total of 3195 independent reflections were refined to $R = 0.0454$. Each Pt^{II} site has the anticipated NO_2Cl square-planar mer coordination. The Pt−N(1) distance (N(1) is the N donor of the $hdta^{4-}$ ligand) is 2.001(9) Å, only slightly shorter than typical Pt−N distances (2.04−2.09 Å) for sp^3 donors. The Pt−O distances to the coordinated glycinato donors in **1** are 2.012(7) and 2.000(8) Å, values very similar to those of *trans*-[Pt(gly)$_2$] (gly = glycinate). The Pt−Cl distance of 2.310(3) Å is in the range of 2.27−2.32 Å observed for other Pt(II)−Cl^- bonds. The bond angles are close to the ideal 90° or 180° value: ∠N−Pt−O = 85.4(3)° and 83.2(4)°; ∠N−Pt−Cl = 176.6(2)°. The $[Pt_2(hdta)Cl_2]^{2-}$ units are packed in an end-to-end fashion such that the [Pt^{II}(iminodiacetate)Cl] headgroups are overlapping. This provides square-planar to square-planar stacking of the headgroups. ^{1}H and ^{13}C NMR data are presented which show that the $[Pt_2(hdta)Cl_2]^{2-}$ coordination of the solid state is maintained in solution. The coordinated glycinato arms of $[Pt_2(hdta)Cl_2]^{2-}$ are equivalent, exhibiting only one AB pattern in the ^{1}H NMR (H_a, 4.31 ppm; H_b, 3.89 ppm; $J_{ab} = 16.1$ Hz) and one type of coordinated carboxylate (^{13}C NMR resonance at 189.7 ppm). Time-dependent ^{1}H and ^{13}C NMR spectra show that inosine first displaces only Cl^- in $[Pt_2(hdta)Cl_2]^{2-}$ in solutions up to one inosine per Pt^{II} center. A higher concentration of inosines (Ino) results in the displacement of one of the glycinato arms, detectable at 175.0 ppm by ^{13}C NMR. The sequential nature and binding of two Ino ligands, necessarily cis in $[Pt_2(hdta)(Ino)_4]$, mimics the steps necessary to allow major groove-spanning ligation of DNA in the manner of the Farrell-type binuclear platinum(II) amine complexes.

Introduction

Crystals of $[MV][Pt_2(hdta)Cl_2]\cdot 4H_2O$ (**1**) (MV^{2+} = methyl viologen or 1,1'-dimethyl-4,4'-bipyridinium, $hdta^{4-}$ = 1,6-hexanediamine-*N*,*N*,*N*',*N*'-tetracetate) contain the following binuclear platinum(II) polyaminocarboxylate:

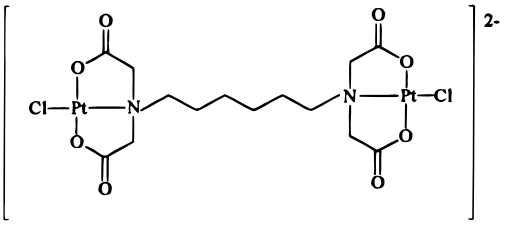

We have recently reported that $[Pt_2(hdta)Cl_2]^{2-}$ reacts with inosine with displacement of Cl^- as a model for the first step in forming interstrand DNA cross-links with this modified cisplatin-like binuclear agent.[1] The interest in $[Pt_2(hdta)Cl_2]^{2-}$ as a possible DNA groove-spanning chelate prompted us to obtain suitable crystals containing $[Pt_2(hdta)Cl_2]^{2-}$ for X-ray diffraction study. The original complex was isolated as a K_2-$[Pt_2(hdta)Cl_2]$ salt, but crystals of X-ray quality could not be obtained for K^+ or a variety of M^{2+} cation replacements such as Ba^{2+}, Zn^{2+}, Ca^{2+}, dimethyldabconium ion, etc. Using the rationalization that stiffer, rodlike dications might improve the likelihood of obtaining crystals of a salt for $[Pt_2(hdta)Cl_2]^{2-}$, we substituted 1,1'-dimethyl-4,4'-bipyridinium ion (methyl viologen, MV^{2+}) by slow growth of the crystalline salt from aqueous solution at 4 °C. Needlelike crystals of $[MV][Pt_2(hdta)Cl_2]\cdot 4H_2O$ were obtained. The crystal and molecular structure of this compound is the central issue of the present paper. The importance of the study resides in the search for binuclear Pt^{II} complexes which act in a fashion now familiar for cisplatin and its derivatives toward DNA and nucleobases.

Cisplatin-like binuclear complexes with two metal binding units connected by an organic tether may be important drugs to overcome acquired resistance and repair pathways which limit cisplatin mononuclear derivatives in antitumor action.[2−12] Their

(1) Lin, F.-T.; Shepherd, R. E. *Inorg. Chim. Acta* **1998**, *271*, 124.

(2) Farrell, N. P. In *Platinum and Other Metal Coordination Compounds in Cancer Chemotherapy*, Howell, S. B., Ed.; Plenum: New York, 1991; pp 81−91.
(3) (a) Farrell, N. P.; Qu, Y.; Van Houghten, B. *Biochemistry* **1990**, *29*, 9522. (b) Roberts, T. D.; Van Houghten, B.; Qu, Y.; Farrell, N. P. *Nucleic Acids Res.* **1989**, *17*, 9719.
(4) Alul, R.; Cleaver, M. B.; Taylor, J.-S. *Inorg. Chem.* **1992**, *32*, 3636.
(5) Schuhmann, E.; Altman, J.; Karaghiosoff, K.; Beck, W. *Inorg. Chem.* **1995**, *34*, 2316.
(6) Farrell, N. P.; Qu, Y.; Hacker, M. P. *J. Med. Chem.* **1990**, *33*, 2179.
(7) Qu, Y.; Farrell, N. *J. Inorg. Biochem.* **1990**, *40*, 255.
(8) Reedijk, J.; Fichtinger-Schepman, A. M.; van Oosterom, A. T.; van de Putte, P. *Struct. Bonding* **1987**, *67*, 53.

10.1021/ic990123o CCC: $18.00
Published on Web 10/02/1999

advantage lies in the formation of interstrand DNA cross-links using N-7 attachments at GG sequences, predominantly.[8−11] It is believed that the tether across the major groove disrupts the binding of repair proteins and proteins utilized for DNA polymerase activity, promoting cytoxicity. Binuclear lesions of DNA may also promote suicide adducts with repair proteins which deplete tumor cells of repair capacity.[13]

There is evidence that some aspects of cisplatin resistance originate with reactions of cisplatin amine complexes with RS^- cellular interceptors such as metallothionein and glutathione.[14−21] Therefore, we have embarked on preparing more protected binuclear Pt^{II} complexes which are linked by tethers to provide the inhibitory effect of interstrand cross-links of binuclear agents toward repair proteins, but with some controls on the reactivity of the metalating headgroup toward cellular nucleophiles. To afford biocompatibility, we have chosen to utilize aminocarboxylate donors for the Pt^{II} center, as these are similar to the protein functionalities and should afford useful H-bonding contacts within the major groove of DNA during the approach of the binuclear agent. The $[Pt_2(hdta)Cl_2]^{2-}$ complex is one of this series of reagents.

Inosine is a useful probe of the action of Pt^{II} agents toward purine bases of DNA,[22−24] because inosine is much more soluble in aqueous solution than guanosine, thus allowing concentration studies in forming Pt^{II} complexes. In our prior report we examined the location of the first substitution process of inosine with $[Pt_2(hdta)Cl_2]^{2-}$. Like other cisplatin-derived agents, the substitution occurs with Cl^- displacement.[1]

In a slower step, a second addition of inosine forms $[Pt_2(hdta)(Ino)_4]$ (**2**), a model for intrastrand cross-links of Pt^{II} antitumor agents which also achieve bidentate GG coordination along both strands of DNA.[3,6,13] This step was not described in our earlier report.[1] Additional NMR information concerning the additional displacement of the glycinato donor is provided in the present study.

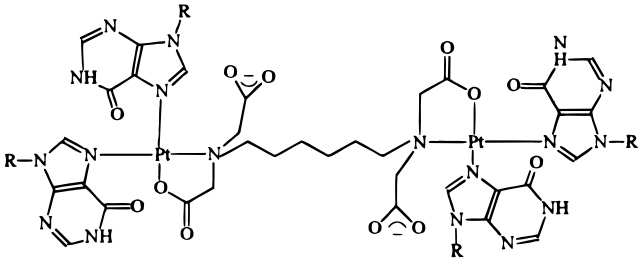

(2)

Experimental Section

Synthesis of $K_2[Pt_2(hdta)Cl_2]$. 1,6-Hexanediamine-*N*,*N*,*N*′,*N*′-tetraacetic acid (H_4hdta) and K_2PtCl_4 were used as supplied by Aldrich. A 0.087 g (2.50×10^{-4} mol) sample of H_4hdta was combined with 0.210 g of K_2PtCl_4 (5.06×10^{-4} mol) in 30.0 mL of deionized water in an Erlenmeyer flask which was protected from room light by an aluminum foil wrap. Operations were performed in subdued room light. The sample was stirred magnetically in a water bath to control the temperature. The pH was adjusted initially to 1.6 with 1.0 M HCl, and the sample was stirred at room temperature for 15 h. It is known from prior studies of platinum(II) aminocarboxylates that, to prevent precipitation of Pt metal or its hydroxides, the first addition of amine donors must be carried out in acidic conditions near a pH of 2.[27−31] The further chelation of carboxylate donors is then carried out by stepwise increases in pH to values near pH 4, and then pH 6. This procedure was adopted in the present work. After the initial 15 h period at pH 1.6, the sample was further heated at pH 1.6 while the temperature was maintained between 55 and 60 °C. The pH was adjusted to 4.0 with 1.0 M KOH. pH measurements were made at 25 °C using a mini combination pH probe and a Fisher Scientific pH meter calibrated with commercial standard buffers. After adjustment to pH 4.0, the sample was heated for 3 h at 55−60 °C with stirring. The pH was then raised with KOH to pH 6.7. The sample was heated with stirring for 1 h at 55 °C. Coordination of carboxylates was indicated by a small drop in pH to 5.5 during the last coordination cycle. The sample was concentrated by rotary evaporation, and the solids were filtered off to yield $K_2[Pt_2(hdta)Cl_2]$. The solid product was recrystallized from hot water to remove KCl with a yield of 55%.

Synthesis of $[MV][Pt_2(hdta)Cl_2]\cdot 4H_2O$. A 2.0 mL sample of water was stirred with the isolated $K_2[Pt_2(hdta)Cl_2]$ salt until saturation was achieved at ca. 35 °C. Heating was provided by suspending a small tube with the sample in a warm water bath. Small amounts of methyl viologen dichloride were added to the warm solution, agitating the contents to achieve mixing and dissolution of the $[MV]Cl_2$ reagent. The clear solution was allowed to cool to room temperature, covered with Parafilm, and placed upright in a refrigerator at 4 °C. After 4 days small needlelike crystals and a large clump of solid crystals were harvested and examined under a microscope. A useful crystal was selected, cleaved for X-ray diffraction, and mounted for study.

Structure Determination. Details of the crystal and data collection are given in Table 3. The cell constants were determined by least-

(9) Bruhn, S. L.; Toney, J. H.; Lippard, S. J. *Prog. Inorg. Chem*. **1990**, *38*, 477.
(10) Cardonna, J. P.; Lippard, S. J. In *Platinum Coordination Complexes in Cancer Chemotherapy*; Hacker, M. P., Douple, E. B., Krakoff, I. H., Eds.; Martinus Nijhoff: Boston, MA, 1984; pp 14−26.
(11) Lippard, S. J. In *Platinum and Other Metal Coordination Compounds in Cancer Chemotherapy*; Howell, S. P., Ed.; Plenum: New York, 1991; pp 1−12.
(12) Hoeschele, J. D.; Kraker, A. J.; Qu, Y.; Van Houghten, B.; Farrell, N. In *Molecular Basis of Specificity in Nucleic Acid-Drug Interactions*; Pullman, B., Jortner, J., Eds.; Kluwer Academic Publishers: Dordrecht, The Netherlands, 1990; pp 301−322.
(13) (a) Van Houghten, B.; Illeyne, S.; Qu, Y.; Farrell, N. *Biochemistry* **1993**, *32*, 11794. (b) Qu, Y.; Farrell, N. *Inorg. Chem*. **1995**, *34*, 3573.
(14) Teicher, B. A.; Holden, S. A.; Herman, T. S.; Sotomayer, E. A.; Khandekar, V.; Rosbe, K. W.; Brann, T.; Korbut, T. T.; Frei, E. *Int. J. Cancer* **1991**, *47*, 252.
(15) Bancroft, D. P.; Lepre, C. A.; Lippard, S. J. *J. Am. Chem. Soc*. **1990**, *112*, 6860.
(16) Bodenner, D. L.; Dedon, P. C.; Keng, P. C.; Borch, R. F. *Cancer Res*. **1986**, *46*, 2745.
(17) Momburg, R.; Bourdeaux, M.; Sarrazin, M.; Charvet, M.; Briand, C. *J. Pharm. Pharmacol*. **1987**, *39*, 691.
(18) Dedon, P. C.; Borsch, R. F. *Biochem. Pharmacol*. **1987**, *36*, 1955.
(19) Norman, R. E.; Sadler, P. J. *Inorg. Chem*. **1988**, *27*, 3583.
(20) Eastman, A.; Barry, M. A. *Biochemistry* **1987**, *26*, 3303.
(21) Odenheimer, B.; Wolf, W. *Inorg. Chim. Acta* **1982**, *66*, L41.
(22) (a) Kong, P.-C.; Theophanides, T. *Inorg. Chem*. **1974**, *13*, 1167. (b) Kong, P.-C.; Theophanides, T. *Inorg. Chem*. **1974**, *13*, 1981.
(23) (a) Hohmann, H.; Helquist, B.; van Eldik, R. *Inorg. Chem*. **1992**, *31*, 1090. (b) Hohmann, H.; Hellquist, B.; van Eldik, R. *Inorg. Chem*. **1992**, *31*, 345.
(24) Suvachittanont, S.; Hohmann, H.; van Eldik, R. *Inorg. Chem*. **1993**, *32*, 4544.
(25) (a) Kortes, R. A.; Lin, F.-T.; Ward, M.; Shepherd, R. E. *Transition Met. Chem.*, in press. (b) Lin, F.-T.; Kortes, R. A.; Shepherd, R. E. *Transition Met. Chem*. **1997**, *22*, 243.
(26) (a) Shepherd, R. E.; Chen, Y.; Zhang, S.; Kortes, R. A. Ru(II)-Polyaminopolycarboxylate Complexes for Improved DNA Probes. In *Electron-Transfer Reactions;* Isied, S., Ed.; Advances in Chemistry Series 253; American Chemical Society: Washington, DC, Chapter 22, pp 367−398.
(27) Kortes, R. A.; Lin, F.-T.; Shepherd, R. E.; Maricondi, C. *Inorg. Chim Acta* **1996**, *245*, 149.
(28) Shepherd, R. E.; Zhang, S.; Kortes, R.; Lin, F.-T.; Maricondi, C. *Inorg. Chim. Acta* **1996**, *244*, 15.
(29) Zheligovoskaya, N. N.; Schelokova, C. R.; Popov, L. V.; Spitsyn, V. I. *Koord. Khim*. **1984**, *10*, 107.
(30) (a) Liu, C. F. *Inorg. Chem*. **1964**, *3*, 680. (b) Erickson, L. E.; McDonald, J. W.; Howie, J. K.; Clow, R. P. *J. Am. Chem. Soc*. **1968**, *90*, 6371.
(31) Hoeschelle, J. D.; Farrell, N.; Turner, W. R.; Richter, C. D. *Inorg. Chem*. **1988**, *27*, 4106.

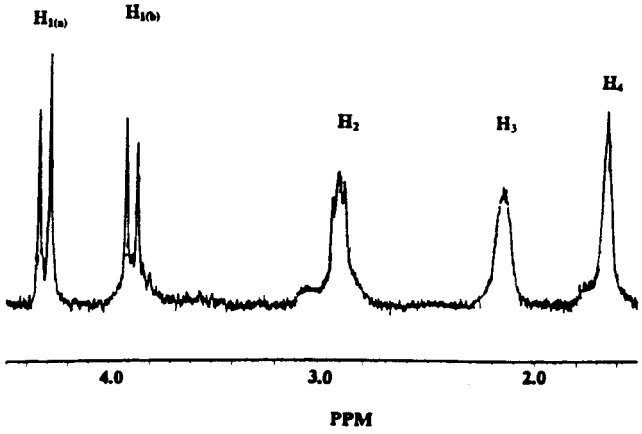

Figure 1. ^{1}H NMR spectrum at 300 MHz for *mer*,*mer*-$K_2[Pt_2(hdta)Cl_2]$ in D_2O at pD 4.5.

squares refinement on diffractometer angles for 25 automatically centered reflections in the range of 20−26° using graphite-monochromated Mo Kα radiation. The data were collected at −65 °C using a Siemens P-3 diffractometer. A total of 2456 independent reflections, uncorrected for absorption, were refined by a full-matrix least-squares method on F^2 using the SHELX crystallographic software package. Two separate crystals from separate syntheses were examined, yielding nearly identical parameters. The better data set gave data that were refined to $R = 0.0454$, [$I > 2\sigma(I)$]. An 0.08 × 0.24 × 0.24 mm light yellow needle of $[MV][Pt_2(hdta)Cl_2]\cdot 4H_2O$ was studied for the reported values. An earlier study had shown that efflorescence of lattice water occurred after 12 h of exposure to the Mo Kα radiation; this prompted the data collection at −65 °C where the problem did not occur.

Instrumentation. The IR spectrum of the isolated product was obtained on a Mattson 100 FT-IR in KBr pellets averaging 32 scans. The ^{1}H NMR data were obtained on AC300 and AM500 Bruker NMR spectrometers using a 12 s delay time. Samples were dissolved in D_2O and adjusted with DCl or NaOD as required for a given experiment. DSS was used as a reference for $\delta = 0.00$. ^{13}C NMR spectra were obtained at 125 MHz on a Bruker AM500 spectrometer using a 40 s delay time. ^{13}C NMR spectra were referenced to 1,4-dioxane's 69.1 ppm resonance. HH-COSY, HC-COSY, and HC-COLOC spectra were obtained on the same instrument.

In ^{1}H NMR and ^{13}C NMR studies of the reaction of $[Pt_2(hdta)Cl_2]^{2-}$ in D_2O with inosine (obtained from Aldrich) several conditions were utilized: With $R = [Pt^{II}_2(hdta)Cl_2]^{2-}$:[inosine], $R \cong 5.0$ (low inosine) and $R \cong 1.0$, 0.50, 0.25, and 0.033 (1:30; high inosine). The time course of the reaction was followed at 20 and 35 °C with equivalent results, except that the 35 °C data could be accumulated more quickly in observing sequential changes. The product complexes under $R = 5.0$, 1.0, and 0.033 were examined by ^{13}C NMR to identify whether coordinated glycinato arms had been displaced by inosine under these differing conditions.

Results and Discussions

The ^{1}H NMR spectrum of $K_2[Pt_2(hdta)Cl_2]$ in D_2O is shown in Figure 1. The 300 MHz ^{1}H NMR parameters are specified in Table 1 according to the following numbering scheme:

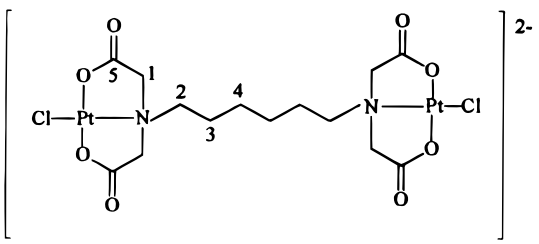

The observed spectrum establishes the symmetrical (*mer, mer*)

Table 1. ^{1}H NMR Parameters for $[Pd_2(hdta)Cl_2]^{2-}$ in D_2O

		$T = 25.0$ °C		$T = 75.0$ °C
		$\Delta\delta^a$	δ (ppm)	δ (ppm)
complex	H_1 (a)	4.31 (d)}^{c} −0.25	4.30 (d)	4.77 (d)}^{d}
	H_1 (b)	3.89 (d)}	3.89 (d)	4.39 (d)}
	H_2	2.91 (t) +0.35	2.90 (t)	3.41 (t)
	H_3	2.14 (br s) −0.34	2.15 (br s)	2.61 (br s)
	H_4	1.65 (br s) −0.75	1.65 (br s)	2.17 (br s)
free ligand^b	H_1	3.85		
	H_2	3.26		
	H_3	1.80		
	H_4	1.40		

^{a} A positive shift ($\Delta\delta$) is an upfield shift. ^{b} Values reported by Aldrich Spectral Library for H_4hdta in D_2O. ^{c} $J = 16.1$ Hz. ^{d} $J = 16.0$ Hz.

Table 2. ^{13}C Chemical Shifts for $[Pt_2(hdta)Cl_2]^{2-}$ in D_2O

	δ (ppm)			δ (ppm)	
carbon	*a*	*b*	carbon	*a*	*b*
C_1	69.5	70.1	C_4	28.8	29.1
C_2	67.9	68.5	carboxylate C	189.5	189.7
C_3	29.3	29.3			

^{a} 35.0 °C; 1,4-dioxane reference at 69.1 ppm. ^{b} 75.0 °C.

type of coordination[32] which is further confirmed by the X-ray diffraction study in a later section of this paper. Only one type of AB glycinato pattern is observed. The center shift (4.10 ppm) is downfield of the free ligand peak as is typical of coordinated glycinato functionalities of Pt^{II} or Pd^{II}. The J_{ab} coupling constant (16.1 Hz) is typical of in-plane glycinates. For comparison, [Pt(edda)] has a J_{ab} of 16.7 Hz.[28] $[Pt(nta)Cl]^-$, which is closely related structurally to the metallo headgroups of $[Pt_2(hdta)Cl_2]^{2-}$, has an AB pattern centered at 4.32 ppm with $J_{ab} = 16.34$ Hz.[27]

The chemical shift pattern of the tether chain follows the same trend as $[Pd_2(egta)Cl_2]^{2-}$.[25,26] The CH_2 nearest the coordinating N shifts upfield upon coordination. The observed $\Delta\delta$ value of +0.35 for this position is similar to the +0.25 value for $[Pd_2(egta)Cl_2]^{2-}$. Further along the tether chain, the CH_2 units experience only downfield shifts of −0.34 for H_3 and −0.25 for H_4 for the hdta complex compared to −0.83 for H_3 in $[Pd_2(egta)Cl_2]^{2-}$.[25a]

All assignments were further established by data collection at 500 MHz at 35.0 and 75.0 °C. The molecule is robust to ligand dissociation; only one type of carboxylato carbon exhibiting a ^{13}C shift at 189.7 ppm indicates that the glycinato donors of $[Pt_2(hdta)Cl_2]^{2-}$ remain coordinated up to 75.0 °C (Figure S-3 in the Supporting Information). However, some thermal instability toward Pt demetalation occurred for samples held for greater than 2 h at 75.0 °C. All ^{1}H NMR resonances shift downfield at 75.0 °C as specified in Table 1. The confirming evidence of the *mer*,*mer* structure was afforded by 2D NMR methods applied at 35.0 and 75.0 °C. The HH-COSY 500 MHz spectrum at 35.0 °C is shown in Figure S-2 in the Supporting Information which clearly establishes the assignments given in Table 1. The HC-COSY 500 MHz spectrum at 35.0 °C (Figure S-3 in the Supporting Information) allows the ^{13}C assignments given in Table 2 where the numbering scheme is the same as for the hydrogens. Additional confirmation was provided by a long-range CH-COLOC spectrum at 35.0 °C (not shown) for the assignments of the glycinato and C_2 carbons.

When the pD of the $[Pt_2(hdta)Cl_2]^{2-}$ sample was raised to ∼10 with NaOD, the glycinato proton's AB set of the (*mer*,*mer*)

(32) (a) Appleton, T. G.; Hall, J. R.; Ralph, S. F. *Inorg. Chem.* **1988,** *24,* 673. (b) Appleton, T. G.; Berry, R. D.; Hall, J. R. *Inorg. Chem.* **1985**, *24,* 666.

Table 3. Crystal Data and Structure Refinement for **1**

identification code	new2
empirical formula	$C_{28}H_{20}CL_2N_2O_{13}Pt_2$
formula weight	1053.54
temperature (K)	200(2)
wavelength (Å)	0.710 73 Å
crystal system	monoclinic
space group	*C*2/*c*
unit cell dimensions	$a = 22.757(5)$ Å, $\alpha = 90°$
	$b = 13.566(3)$ Å, $\beta = 109.07(3)°$
	$c = 12.120(2)$ Å, $\gamma = 90°$
volume (Å^3), *Z*	3536.4(12), 4
density (calcd) (Mg/m^3)	1.949
absorption coefficient (mm^{-1})	8.116
F(000)	1984
crystal size (mm)	0.08 × 0.24 × 0.24
θ range for data collection (deg)	1.77−25.02
limiting indices	$0 \le h \le 27$, $0 < k \le 16$, $-14 \le l \le 13$
no. of reflections collected	3195
no. of independent reflections	3115 ($R_{int} = 0.0430$)
completeness to $\theta = 25.02°$ (%)	99.6
absorption correction	empirical
max and min transmission	1.0000 and 0.0001
refinement method	full-matrix least-squares on F^2
no. of data/restraints/parameters	3115/0/271
goodness-of-fit on F^2	0.959
final *R* indices [$I > 2\sigma(I)$]	Rl = 0.0454, wR2 = 0.1157
R indices (all data)	Rl = 0.0648, wR2 = 0.1291
largest diff peak and hole (e Å^{-3})	1.152 and −1.232

coordinated Pt^{II} sites collapsed into a singlet at 3.87 ppm whereas the backbone resonances at 2.90, 2.13, and 1.65 ppm for H_2, H_3, and H_4 protons remained virtually unchanged. This is consistent with H/D exchange at higher pD values for coordinated glycinato donors which occurs much more rapidly than that in pendant carboxylates.[32]

^{195}Pt NMR Spectrum. The ^{195}Pt NMR spectrum (published elsewhere[1]) of $[Pt_2(hdta)Cl_2]^{2-}$ confirms the presence of a chloride as the fourth in-plane ligand. Only one ^{195}Pt signal is observed at −1330 ppm vs Na_2PtCl_6 at 35.0 °C. The same donor set for each Pt^{II} site in $[Pt_2(hdta)Cl_2]^{2-}$ is present in *mer*-[Pt(mida)Cl]$^-$ according to the symmetry shown by the ^{1}H and ^{13}C NMR spectra. A sample of the K^+ salt of *mer*-[Pt(mida)Cl]$^-$ (mida^{2-} = *N*-methyliminodiacetate) was observed to have a ^{195}Pt resonance at −1317 ppm. This confirms the presence of Cl^- since loss of Cl^- and replacement by H_2O would produce a species which resonates over 200 ppm further from $PtCl_6^{2-}$, e.g., near −1130 ppm. No resonance was detected in this region. Hence, both Pt^{II} atoms have equivalent NO_2Cl coordination as required by the symmetry aspects of the molecule already noted for ^{1}H and ^{13}C resonances.

Infrared Spectrum. The IR spectrum of $K_2[Pt_2(hdta)Cl_2]$ in KBr exhibited only one type of carboxylate stretch at 1642 cm^{-1}, indicative of fully coordinated carboxylates as required by ^{13}C NMR data. For comparison, [Pt(edda)] (edda^{2-} = ethylenediamine-*N*,*N*′-diacetate) exhibits the same stretch at 1640 cm^{-1}.[28]

Structure of [MV][Pt$_2$(hdta)Cl$_2$]·4H$_2$O. The data collection methods and crystal information are summarized in Table 3 and are discussed in the Experimental Section. The ORTEP diagram of the [methyl viologen][$Pt_2(hdta)Cl_2$] cation/anion pair is shown in Figure 2, and the molecular packing diagram is presented in Figure 3. Selected bond distances and angles are summarized in Table 4.

Additional supporting crystallographic data are deposited as Supporting Information. These include Table S-1, atomic coordinates and equivalent isotropic displacement parameters; Table S-2, complete list of bond lengths and bond angles for [MV][$Pt_2(hdta)Cl_2$]·4H_2O (**1**); Table S-3, anisotropic displacement parameters for **1**; and Table S-4, hydrogen coordinates and isotropic displacement parameters.

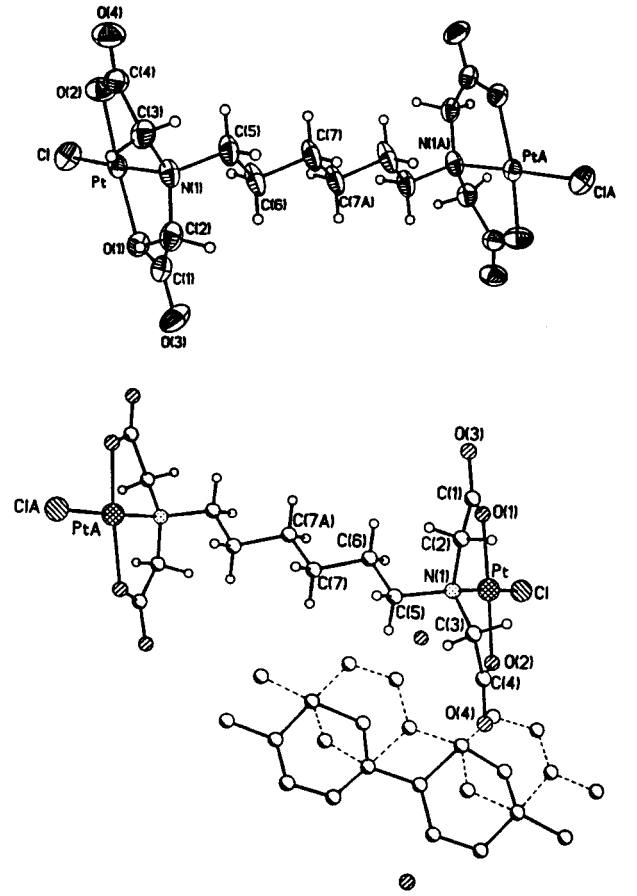

Figure 2. Crystal structure of the [MV][$Pt_2(hdta)Cl_2$] ion pair showing the disordered MV^{2+}positions.

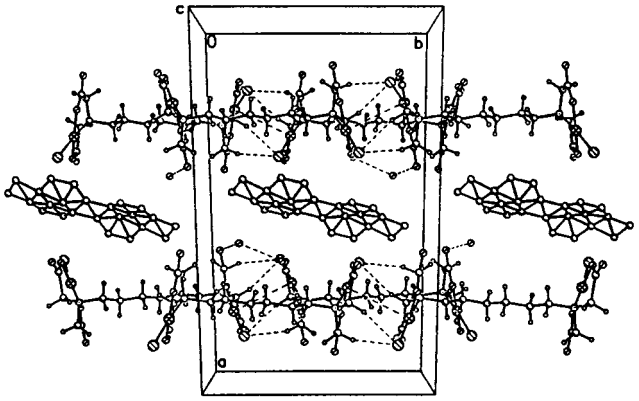

Figure 3. Molecular packing and unit cell for **1**.

The anion/cation pair for [MV][$Pt_2(hdta)Cl_2$] in Figure 2 shows the disorder of the MV^{2+} cation which shifts between two locations along a translation axis between $[Pt_2(hdta)Cl_2]^{2-}$ and the next row of $[Pt_2(hdta)Cl_2]^{2-}$ ions. The flexible rotation along the 4,4′-bond of the methyl viologen dication also introduces twisting and apparent distortions into the atom positions of the MV^{2+} ion. The more important structure of the $[Pt_2(hdta)Cl_2]^{2-}$ ion is clearly resolved. Each Pt^{II} center possesses the mer coordination similar to *mer*-[Pt(mida)Cl]. The Pt^{II} headgroups alternate, one pointing out of the approximate plane of the hexamethylene chain and the other Pt^{II} center pointing behind the same place. This orientation has further ramifications observed in the molecular packing of the $[Pt_2(hdta)Cl_2]^{2-}$ units such that square-planar to square-planar stacking occurs between subunits which project inward and

Table 4. Selected Bond Distances and Bond Angles for $[MV][Pt_2(hdta)Cl_2]\cdot 4H_2O$[a]

Pt−N(1)	2.001(9)	Pt−O(2)	2.000(8)
Pt−O(1)	2.012(7)	Pt−Cl	2.310(3)
O(1)−C(1)	1.269(13)	N(1)−C(3)	1.484(13)
N(1)−C(2)	1.491(15)	N(1)−C(5)	1.534(12)
		C(1)−C(2)	1.523(15)
C(1)−O(3)	1.234(13)	C(3)−C(4)	1.510(17)
O(2)−C(4)	1.282(15)	C(5)−C(6)	1.524(15)
N(1)−Pt−O(2)	83.2(4)	N(1)−Pt−O(1)	85.4(3)
O(2)−Pt−O(1)	167.6(3)	N(1)−Pt−Cl	176.6(2)
O(2)−Pt−Cl	96.6(3)	O(1)−Pt−Cl	95.1(2)
C(1)−O(1)−Pt	111.2(7)	C(3)−N(1)−C(2)	115.4(9)
C(3)−N(1)−Pt	105.2(7)	C(3)−N(1)−C(5)	111.6(8)
O(3)−C(1)−C(2)	119.8(11)	C(4)−O(2)−Pt	113.5(8)

[a] Bond lengths in angstroms and bond angles in degrees.

outward of adjacent $[Pt_2(hdta)Cl_2]^{2-}$ units. This provides an interlocked stacking structure in a series of units somewhat like a series of N's would achieve if printed consecutively and overlapping along a line. A model of the face-to-face stacking assembly showed upon inspection that the Pt^{II} center resides above the N(1) donor of the stacking partner. Thus, the Pt^{II} complexes are not directly above one another, and the repulsions along the "z" direction perpendicular to the individual square planes of the Pt^{II} centers are avoided.

The Pt^{II} headgroups of $[Pt_2(hdta)Cl_2]^{2-}$ are each approximately square-planar. The Pt−N(1) distance, where N(1) is the terminal nitrogen donor from the $hdta^{4-}$ ligand, is 2.001(9) Å. This is slightly shorter than typical Pt−N distances to other sp^3 N donors which have a range of 2.04−2.09 Å.[33−36] The shortening of the Pt−N(1) distance is enforced by the chelation of the two glycinato donor groups which have rather normal Pt−O distances of 2.012(7) Å for O(1) and 2.000(8) Å for O(2). The Pt−Cl distance of 2.310(3) is well within the range of 2.27−2.32 Å observed in complexes with Pt(II)−Cl^- bonds.[33,34,37,38] The chelation enforces a slight distortion from the idealized 90° angles. The N(1)−Pt−O(1) and N(1)−Pt−O(2) angles are 85.4(3)° and 83.2(4)°, respectively, the effect of strain introduced by the glycinato chelation withholding the reach of the chelate arms from the ideal 90° value. Freeman and Golomb have described the bis glycinato complex *trans*-$[Pt(gly)_2]$.[39] The similarity of the bonding parameters for the *trans*-$[Pt(gly)_2]$ complex and the headgroup of $[Pt_2(hdta)Cl_2]^{2-}$ is readily seen as presented in the diagram below:

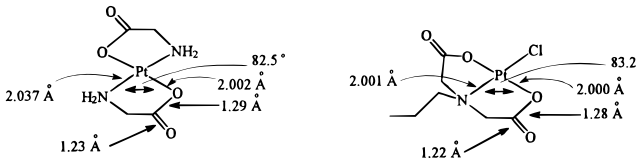

Freeman and Golomb point out that the interior angle for a coordinated glycinato group will be theoretically 83° if the Pt(II)−N bond is 2.0 Å.[36] Both the glycinato complex and the Pt^{II} headgroups of **1** of this paper hold to the predicted value. The N−(1)−Pt−Cl angle of 176.6(2)° is very near the anticipated linear configuration. All the bond distances and angles along the intervening methylene chain are the normal 1.52 Å and 109°. The structure shown in Figure 3 confirms all of the conclusions based on ^1H and ^{13}C NMR for the structure of $[Pt_2(hdta)Cl_2]^{2-}$. Therefore, the species isolated in **1** remains intact in solution; e.g., the glycinato donors remain coordinated (Figure S-1).

The molecular packing structure (Figure 3) shows more clearly the placement of the MV^{2+} cations. Although disordered along the translation axis between the $[Pt_2(hdta)Cl_2]^{2-}$ chains, the MV^{2+} dictations are slightly rotated to place one methylpyridinium cation unit pointing toward the region of stacked Pt^{II} headgroups. This is the location of greatest net negative charge. The opposite methylpyridinium center faces another face-to-face Pt^{II} stacking arrangement on the opposite chain. There are solvent H_2O molecules near the glycinato carbonyl oxygens. Additional associations, based on the nearness of atoms, are detectable between the chloride of one Pt^{II} center with the glycinato methylene unit of the next door neighbor provided by the adjacent Pt^{II} of the pair of headgroups which are intertwined in the aforementioned stacking pattern. All of the H-bonding contacts help to enforce the crystal stacking which creates the groove in which the MV^{2+} counterions reside. The complex pattern of the molecular stacking, together with the electrostatic cross-linking provided by the MV^{2+} groups, strongly suggests the reason for the absence of highly ordered, crystalline materials when MV^{2+} is replaced by more spherical point charges such as K^+ or Ba^{2+}. The more spherical ions cannot form suitable electrostatic bridges. The latter salts did not provide crystalline products suitable for X-ray diffraction.

Addition of Inosine. The ^1H NMR spectrum of inosine exhibits characteristic features with chemical shifts (ppm) of 8.31 (s) for the H-8 ring proton, 8.18 (s) for the H-2 ring proton, and 6.065 (d) for the sugar proton on the carbon attached to the purine, H_1', and triplets for H_2' (4.75 ppm) and H_3' (4.44 ppm), a doublet at 4.18 ppm for H_4', and a quartet for H_5' at 3.90 ppm. The notation refers to the standard numbering assignments in the following drawing:

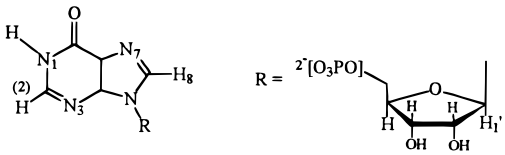

The resonance at 8.31 ppm decreases with time in D_2O, which assigns this proton as H-8 since purines undergo H/D exchange at this position.[22] When inosine is combined with $[Pt_2(hdta)Cl_2]^{2-}$ in D_2O at 20 °C at the ratio of ca. 2.5:1.0 inosine per Pt^{II} center (5 inosines:complex), the effect of inosine coordination is soon apparent. The spectrum at first appears as the sum of the spectra of free inosine and $[Pt_2(hdta)Cl_2]^{2-}$ (see Figure 4A). However, within 30 min coordination of the purine base is clearly evidenced by new resonances appearing at 8.82 and 8.25 ppm and a small doublet at 6.17 ppm. These are, respectively, the protons H-8, H-2, and H_1' for the coordinated inosine ligand. Both protons of the purine ring exhibit a downfield shift upon coordination. The influence on the H-8 proton is larger ($\Delta\delta$ = −0.56 ppm) compared to −0.10 for H-2. Kong and Theophanides reported that the bis inosine adduct of cisplatin, *cis*-$[Pt(NH_3)_2$-

(33) Rochon, F. D.; Dong, P.-C.; Melanson, R.; Skov, K. A.; Farrell, N. *Inorg. Chem.* **1991**, *30*, 4531.
(34) Unakoski, K.; Kinoshita, I.; Fudai-Yusuba, Y.; Matsumoto, K.; Ooi, S.; Nakai, H.; Shiro, M. *J. Chem. Soc., Dalton Trans.* **1989**, 815.
(35) Lippert, B.; Lock, C. J. L.; Speranzini, R. A. *Inorg. Chem.* **1981**, *20*, 335.
(36) Bitha, P.; Morton, G. O.; Dunne, T. S.; Delos Santos, E. F.; Lin, Y.; Boone, S. R.; Haltiwanger, R. C.; Pierpont, C. G. *Inorg. Chem.* **1990**, *29*, 645.
(37) Cheng, L.-K.; Yeung, K.-S.; Che, C.-M.; Cheng, M.-C.; Wany, Y. *Polyhedron* **1993**, *12*, 1201.
(38) Beusichem, M. V.; Farrell, N. *Inorg. Chem.* **1992**, *31*, 1880.
(39) Freeman, H. C.; Golomb, M. L. *Acta Crystallogr., Sect. B* **1969**, *25*, 1203.

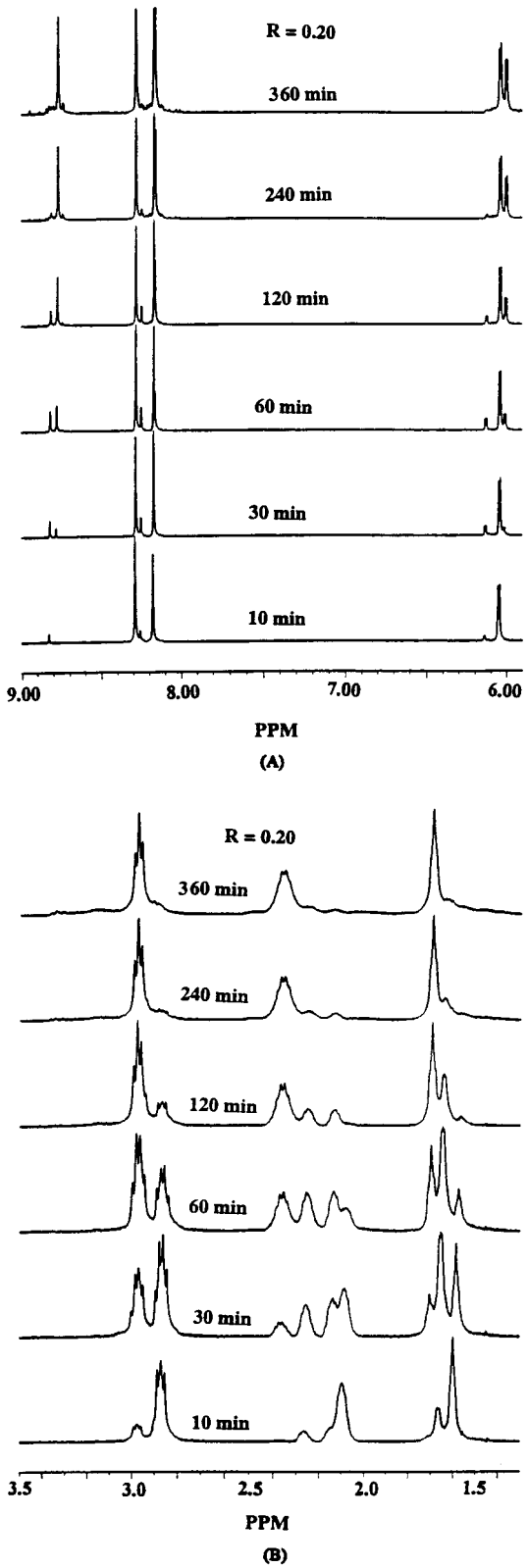

Figure 4. Time dependence of the $[Pt_2(hdta)Cl_2]^{2-}$/inosine reaction at $R = 0.20$ monitored by ^1H NMR at 35 °C: (A) purine base region at times of 10, 30, 60, 120, 240, and 360 min, (B) backbone tether region at 10, 30, 60, 120, 240, and 360 min.

$(Ino)_2]^{2+}$, shows downfield shifts of −0.81 ppm for H-8 and −0.38 ppm for H-2.[22a] A larger influence of the cationic $[Pt(NH_3)_2]^{2+}$ fragment compared to the neutral $[Pt^{II}$−iminodiacetate] functionality of $[Pt_2(hdta)]$ is expected since the downfield shift originates in large part from the σ withdrawing effect of the metal center. Carboxylates neutralize the charge at the Pt^{II} center to a greater extent than NH_3 ligands. The greater shift of the H-8 proton clearly indicates the site of Pt^{II} attachment to inosine is at N-7. The same evidence has been given for N-7 coordination of cisplatin to inosine.[22a] When the [inosine]:Pt^{II} site ratio exceeds 1:1, a slower substitution reaction occurs, forming a new species. This species is detected with resonances slightly upfield of the first coordinated species' shifts for the purine and H_1' sugar protons at 8.78, 8.19, and 6.01 ppm. As the new species forms, there is a corresponding two-step shift of the tether backbone resonances, moving downfield at 3.03 ppm (H-2), 2.47 ppm (H-3), and 1.75 ppm (H-4) as seen in Figure 4B. This indicates formation of bis N-7 inosine adducts at the Pt^{II} sites at longer times.

Because of the importance of the nature of the sequential steps in which the *mer*-$[Pt^{II}(mida)Cl]$-like headgroups of $[Pt_2(hdta)Cl_2]^{2-}$ add additional purines, the addition of inosine was more carefully studied at near physiological conditions (35 °C) at three ratios of [complex]:[inosine], $R = 5.0$, 1.0, and 0.033, at 500 MHz by ^1H NMR. If complexes such as $[Pt_2(hdta)Cl_2]^{2-}$ were to be useful antitumor agents, three features would be important: (1) the Cl^- group should be rapidly displaced, or with aquation, the resulting $Pt^{II}-OH_2$ species should be rapidly displaced by the inosine (a stand-in for guanosine); (2) a second reaction should occur with additional purine bases which would represent the analogous reaction to become bidentate GG chelation along a DNA strand; (3) it is also preferable that the ligand addition should stop when two purines bind the Pt(II) center.

The first experiments were performed at $R \approx 0.033$ (a large excess of inosine). The rapid evolution of the first addition product via displacement of Cl^- or H_2O (which will be shown later) is observed within 5 min and more clearly at 8 min (Figure S-4). With time, the second addition commences. New signals at 8.78 ppm for H-8 appear (Figure S-4) at 30 min, upfield of the initial adduct at 8.82 ppm. Due to the high concentration of inosine free ligand, it was easier to observe these changes rather indirectly by examining the changing features of the $(CH_2)_n$ protons of the tether between the metal centers. This is presented in Figure S-5 where the resonances left to right are those of $NCH_2(2)$, $CH_2(3)$, and $CH_2(4)$ with data collection at 5, 8, 20, 30, 60, and 180 min. The $[Pt_2(hdta)Cl_2]^{2-}$ resonances at 5 min begin to decrease while a second species with respective resonances more downfield for the three sets of protons at positions 2, 3, and 4 (see the drawing for numbering) show increases. This reaction continues throughout the first hour, but a third complex is clearly detectable within 20 min. The third species, which will be shown to be the bis adduct, completely consumes both the starting complex, $[Pt_2(hdta)Cl_2]^{2-}$, and its first addition product, $[Pt_2(hdta)(Ino)_2]$, within 3 h.

The above experiment was repeated at $R \cong 0.20$. The growth of the first addition product is shown for the purine ring region in Figure 4A and for the matching times in the tether backbone region in Figure 4B. The reaction forming $[Pt_2(hdta)(Ino)_4]$ bis adducts at each Pt^{II} center is complete in about 3 h (between the two scans at 2 and 4 h) whereas the initial $[Pt_2(hdta)(Ino)_2]$ product is maximal between 30 and 60 min. Its amplitude is already decreasing after 30 min. Both the purine region (4A) and tether backbone region (4B) indicate the influence of coordination of the first one, and then two inosines per Pt^{II} center.

The progressively downfield shift of the tether H-3 and H-4 backbone resonances from the starting values for $[Pt_2(hdta)Cl_2]^{2-}$ to the intermediate case of $[Pt_2(hdta)(Ino)_2]$, and finally $[Pt_2(hdta)(Ino)_4]$, is seen most easily for the spectra at 30 and 60

min for the backbone region (Figure 4B). The stepwise downfield shifts of H-3 and H-4 implicate a progressively higher effective positive charge on the Pt^{II} center with sequential additions of inosine. This is consistent with the first displacement of anionic Cl^- from the starting complex, and importantly, the second addition of inosine must displace a coordinated glycinato donor. This step also removes a negatively charged group, increasing the withdrawing capacity of the Pt^{II} center. Thus, downfield shifts occur as monitored by the effects along the tether chain. The $NCH_2(2)$ position is least sensitive to the second addition. Its resonances are unchanged except for the splitting pattern which becomes a simple triplet at 2.96 ppm for $[Pt_2(hdta)(Ino)_4]$, but appears as a quartet for $[Pt_2(hdta)(Ino)_2]$. $CH_2(3)$ and $CH_2(4)$ are more sensitive with $[Pt_2(hdta)(Ino)_2]$ having shifts at 2.25 ppm for $CH_2(3)$ and 1.63 ppm for $CH_2(4)$. These then change into 2.39 for $CH_2(3)$ and 1.70 for $CH_2(4)$.

The H-8 position moves from 8.82 ppm for $[Pt_2(hdta)(Ino)_2]$ to 8.78 ppm for $[Pt_2(hdta)(Ino)_4]$; H-2 changes from 8.24 to 8.25 ppm for this change, and H_1' switches from 6.13 to 5.99 ppm.

^{13}C NMR Data for the Inosine Reaction. Additional proof of the ability of $[Pt_2(hdta)Cl_2]^{2-}$ to add sequentially by one and then two inosines per Pt^{II} site is given in Figure S-6 for the ^{13}C NMR data collected under $R = 5.0$, 0.50, and 0.033 conditions corresponding to Pt^{II} in excess, Pt^{II} equivalent, and inosine in excess conditions. The ^{13}C resonances in the 170−190 ppm region are the diagnostic part of these spectra, taken after 6 h for complete reaction. When Pt^{II} is in excess, only bound glycinato resonances appear at 189.7 and 188.5 ppm (Figure S-6A) for the starting $[Pt_2(hdta)Cl_2]^{2-}$ complex and $[Pt_2(hdta)(Ino)_2]$, respectively. At $R = 0.5$, which is one inosine per Pt^{II} center, all the Pt^{II} sites are converted to the 188.5 ppm resonances for $[Pt_2(hdta)(Ino)_2]$ (in Figure S-6B). When inosine is in large excess, the relative intensity of carbons from the complex is lowered. However, a signal at 175 ppm of comparable intensity to another at 188.5 ppm (Figure S-6C) demonstrates that each Pt^{II} center *has one glycinato group bound, and one displaced*, in forming $[Pt_2(hdta)(Ino)_4]$. The bis inosine complexes should have differentiable inosine ligands, one trans to the N(1) donor and a second inosine cis to the N(1) donor. Yet only one chemical shift is observed for either H-8 or H-2 of the inosine ring, and the ^{13}C NMR data unambiguously identify steps which lead to the addition of one inosine without displacement of a glycinato donor at the Pt(II) center, and a second addition that occurs with the displacement of one glycinato donor, but not both. The only interpretation possible is that the electronic changes which prompt the reverse upfield shift are more significant in determining the chemical shifts for coordinated bis inosine H-8 and H-2 protons than are differences due to trans effects as perturbations to the dominate effect of net charge at the Pt(II) center.

Conclusions

The structure of $[Pt_2(hdta)Cl_2]^{2-}$ is the anticipated mer, mer arrangement as shown by the crystal structure of the $[MV][Pt_2(hdta)Cl_2]\cdot 4H_2O$ salt. ^{1}H, ^{13}C, and ^{198}Pt NMR data have shown that the coordination at Pt(II) in **1** is maintained in aqueous solution.

One important observation with inosine as an entering purine base is that the first addition is rapid for the displacement of Cl^- (reaction approaching completion within 60 min). The first substitution step first-order rate constant is independent of inosine concentration over a 20-fold range from $R = 4.0$ (Pt^{II} in excess)[1] to $R = 0.20$ (inosine in excess). But the second addition of another inosine at the same Pt^{II} site has already commenced at a significant rate depending upon the inosine concentration for R near 0.20 before 60 min of reaction time has been reached. The rate constant for the first step is 3.48×10^{-4} s^{-1}.[1] For the second addition step, a second-order constant of 3.7×10^{-3} M^{-1} s^{-1} is calculated from the NMR data at $R = 0.20$.

Current data for substitution of purine nucleobases, water, and thiolato ligands on Pt^{II} complexes related to cisplatin have provided evidence that the substitution process is an associative interchange substitution mechanism (I_a) in character.[40−47] The displacement of the Cl^- leaving group by an entering ligand X proceeds through a distorted trigonal bipyramidal intermediate in which the entering ligand varies in the extent of bond making that assists weakening of the $Pt^{II}-Cl^-$ bond. Structures relevant to the loss of Cl^- in cisplatin or in $[Pt^2(hdta)Cl_2]^{2-}$ at each Pt^{II} headgroup may be pictorially represented as in the figure where X is an entering ligand and L′ represents other donors within the original Pt^{II} complex's donor set (L′ = NH_3 or Cl^- in cisplatin, carboxylate in the $[Pt_2(hdta)Cl_2]^{2-}$, and $-NH_2$ in $[Pt(dien)Cl]^+$):

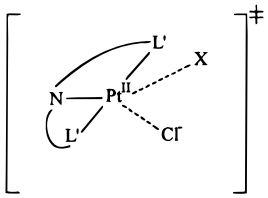

Second-order reaction kinetics are exhibited by the good thiolato nucleophiles (X = glutathione, cysteine, metallothionein),[40−43] but for poorer nucleophiles including purine bases, the substitution process adopts a solvolysis-controlled pathway.[44−46] The rates of substitution of 5′-GMP are deceptively independent of 5′-GMP concentration that might be taken as a dissociative pathway.[44−46] But the even 10^4 slower pathway for the loss of Cl^- without the presence of purine bases points to their initial involvement in the displacement of Cl^- in a $Pt^{II}-Cl^-$ bond of cisplatin-related ligands. The absence of a concentration dependence for substitution by purines on Pt−Cl bonds can be reconciled if the initial five-coordinate intermediate formed with X = purines in a I_a-type intermediate is substitutionally labile and favoring displacement of the entering purine by water in the activated complex. The resultant aqua-associated intermediate may then dissociate Cl^-, and the species with Cl^- dissociated (either as an aqua$-Pt^{II}$ complex or as an ion pair with the departed Cl^-) then reacts with the purine base, retained in the nearby solvation sphere, to complete the substitution event. By contrast, the RS^- nucleophiles produce more strongly coordi-

(40) Johnson, N. P.; Hoeschele, J. D.; Rahn, R. O. *Chem. Biol. Interact*. **1980**, *30*, 151.
(41) Repta, A. J.; Long, D. F. In *Cisplatin Current Status and New Developments*; Pretayko, A. W., Crooke, S. T., Carter, S. K., Eds.; Academic Press: New York, 1980; p 185.
(42) Corden, B. *Inorg. Chim. Acta* **1987**, *137*, 125.
(43) Andrews, P. A.; Murphy, M. P.; Howell, S. B. *Mol. Pharmacol*. **1986**, *30*, 643.
(44) Djuran, M. I.; Lempers, E. L. M.; Reedijk, J. *Inorg. Chem.* **1991**, *30*, 2648.
(45) Guo, Z.; Chen, Y.; Zang, E.; Sadler, P. J. *J. Chem. Soc., Dalton Trans.* **1997**, 4107.
(46) Guo, Z.; Sadler, P. J.; Zang, E. *J. Chem. Soc., Chem. Commun*. **1997**, 27.
(47) (a) Bose, R. N.; Moghaddas, S.; Weaver, E. L.; Cox, E. H. *Inorg. Chem*. **1995**, *34*, 5878. (b) Slavin, L. L.; Cox, E. H.; Bose, R. N. *Bioconjugate Chem*. **1994**, *5*, 316.

nated I_a intermediates. These intermediates with $X = RS^-$ are not solvent labile, and proceed directly to the Pt−SR bound product with second-order kinetics.[44]

Our results for the first addition step with inosine on $[Pt_2(hdta)Cl_2]^{2-}$ are comparable to those of the research studies of Reedijk et al.[44] and Sadler et al.[45,46] on the substitution of 5′-GMP with $[Pt(dien)Cl]^+$. Rate constants for the first addition of 5′-GMP to $[Pt(dien)Cl]^+$ have been reported to be 0.62×10^{-4} s^{-1},[44] 1.4×10^{-4} s^{-1},[45] and ca. 1.0×10^{-4} s^{-1}.[47] The related first step for binding $[Pt(NH_3)_2Cl_2]$ to a G base of DNA has been measured with a rate constant of 1.02×10^{-4} s^{-1}.[48] These values are all very comparable to the rate constant with the purine base inosine with $[Pt_2(hdta)Cl_2]^{2-}$ (3.48×10^{-4} s^{-1}) of this work. It also is consistent with an I_a-type substitution process that the π-donating carboxylate groups of the $htda^{4-}$ ligand (L′ ligands in the above intermediate pictorial representation), cis to the leaving Cl^-, would modestly accelerate the rate of displacement of Cl^- relative to the *cis*-amines of dien in $[Pt(dien)Cl]^+$. Lippard and co-workers report the half-life for forming the first Pt−G bond on DNA as 1.9 ± 0.1 h[48] compared to the displacement of Cl^- by inosine on $[Pt_2(hdta)Cl_2]^{2-}$ of 0.3 h of this work. The electrostatic environment and solvation for Pt^{II} substitution on the DNA polymer is surely different from processes in homogeneous solution, but the evidence here supports the idea that these factors do not make a significant difference in the mechanism or rates of substitution on Pt^{II} complexes which are dominated by aspects of bond formation in the I_a intermediate.

The second step in forming the bidentate adduct on DNA was measured by Lippard's research group as having a first-order rate constant of 9.2×10^{-5} s^{-1} ($t_{1/2} = 2.1 \pm 0.3$ h).[48] Since our study is in homogeneous solution between free inosine rather than a nearby tethered G base of the GG unit along a DNA strand as in the Lippard study, we must convert the second-order rate constant of 3.7×10^{-3} M^{-1} s^{-1} for the substitution of the second inosine per Pt^{II} site of $[Pt_2(hdta)(Ino)_2]$ to a pseudo-first-order rate constant under the conditions of our reaction to make any comparison. The NMR data were collected under reaction conditions for the second step wherein $[Ino]_{av} = 0.050$ M during the substitution process. Hence, the calculated comparison rate constant of 1.9×10^{-4} s^{-1} is obtained. Again, the rates of substitution are very similar for the formation of $[Pt_2(hdta)(Ino)_4]$ with the substitution of inosine occurring 2−3 times faster than for the second G base of the GG pair of DNA with the monobound cisplatin complex.

It has been pointed out to us that the opening of a chelate ring at the metallo headgroup of $[Pt_2(hdta)Cl_2]^{2-}$ at a G base site of DNA requires more space than for cisplatin. The inference is that the polyaminocarboxylate headgroup is too large to afford complexation at a G base of DNA, and that this problem would eliminate the consideration of Pt^{II}(pacs) as antitumor agents. Molecular models of complexes easily show that the size of the Pt^{II} headgroup of $[Pt_2(hdta)Cl_2]^{2-}$ is smaller than the headgroups of related $[Ru^{III}(edta)(H_2O)]^-$ or $[Ru(H_2cydta)Cl_2]$ complexes,[49] and much smaller than the headgroups of the polypyridyl-type Ru^{II} complexes such a $[Ru(bpy)_2Cl(H_2O)]^+$ and $[Ru(terpy)(bpy)(H_2O)]^{2+}$,[50,51] which are all well-known to coordinate to N-7 bases of DNA in the major groove. The physical size constraints are not restrictive of molecules such a $[Pt_2(hdta)Cl_2]^{2-}$ as potential antitumor agents. To the contrary, there is ample room for their coordination of suitable locations along a DNA strand based on the evidence of prior larger DNA metallo-derivatizing agents as models.

A second concern that was raised by a reviewer is whether there would be considerable restriction to rotation if the Pt_2(hdta) chromophore were locked into place across the major groove by binding on opposite strands through G bases. The concern is that there would be steric blocking of the second substitution event. An examination of a model of Pt_2(hdta) attached to one G base shows that only minor displacements of one of the glycinato in-plane arms is required to open up the second coordination site. The ability of the headgroup to contort in a fashion needed to provide proximity to the incoming second G base would appear no more severe than the motions required to allow bidente GG coordination to DNA than has already been shown to occur with the Farrell-type dinuclear complexes.[2−7] Examination of the model shows that the pendant glycinato arm can easily fold back away from the coordination position of the second G base, and can be nearly coparallel with the tether chain, out of the way of coordination. Also, the DNA lesions with $[Ru^{III}(edta)]^-$ and $[Ru^{III}(cydta)]^-$ have such pendant glycinato units even for the first A or G adduct. The presence of a pendant glycinato moiety does not prevent coordination of these larger metallo headgroups.[49]

Clearly, the work reported here is only a first step toward utilization of Pt(pacs) as antitumor agents, and other structural modifications are sure to afford other advantages such as solubility and cell-transport capabilities.

Acknowledgment. We gratefully acknowledge prior Research Corporation support for a 3 month research fellowship for R.A.K. and general support of the research program of R.E.S.

Supporting Information Available: Tables S-1−S-4 giving atomic coordinates, complete lists of bond angles and lengths, and anisotropic displacement factors and Figures S-1−S-6 showing HH-COSY, HC-COSY, and ^{13}C NMR spectra of $[Pt_2(hdta)Cl_2]^{2-}$ and ^1H NMR kinetic data for substitution of inosine at $R = 0.033$ and a ^{13}C NMR product analysis at $R = 5.0$ of $[Pt_2(hdta)(Ino)_4]$. This material is available free of charge via the Internet at http://pubs.acs.org.

IC990123O

(48) Bancroft, D. P.; Lepre, C. A.; Lippard, S. J. *J. Am. Chem. Soc*. **1990**, *112*, 6860.

(49) (a) Chatterjee, D.; Bajaj, H. C.; Das, J. *J. Chem. Soc., Dalton Trans*. **1995**, 2497. (b) Vilaplana, R. A.; Gonzales-Vilchez, F.; Ruiz-Valero. *Inorg. Chim. Acta*. **1994**, *224*, 15.

(50) (a) Sitlani, A.; Long, E. C.; Pyle, A. M.; Barton, J. K. *J. Am. Chem. Soc*. **1992**, *114*, 2303. (b) Pyle, A. M.; Barton, J. K. *Prog. Inorg. Chem*. **1990**, *38*, 413. (c) Barton, J. K.; Lolis, E. *J. Am. Chem. Soc*. **1985**, *107*, 708.

(51) Grover, N.; Gupta, N.; Thorp, H. H. *J. Am. Chem. Soc.* **1992**, *114*, 3390.